

Supporting information

Towards photovoltaic windows: Scalable fabrication of semitransparent modules based on non-fullerene acceptors via laser-patterning

Enrique Pascual-San-José^{a,b}, Golnaz Sadoughi^c, Luca Lucera^c, Marco Stella^b, Eugenia Martínez-Ferrero^b, Graham E. Morse^c, Mariano Campoy-Quiles*^a and Ignasi Burgués-Ceballos*^c

^a Institut de Ciència de Materials de Barcelona (ICMAB-CSIC), Campus de la UAB, 08193, Bellaterra, Barcelona, Spain.

^b EURECAT, Centre Tecnològic de Catalunya, Parc Científic i de la Innovació TecnoCampus, Av. Ernest Lluch, 36, 08302, Mataró, Barcelona, Spain.

^c Merck Chemicals Ltd., Chilworth Technical Centre, University Parkway SO16 7QD Southampton, UK.

*Address all correspondence to Dr. Mariano Campoy-Quiles (mcampoy@icmab.es) and Dr. Ignasi Burgués-Ceballos (ignasi.burgues@icfo.eu)

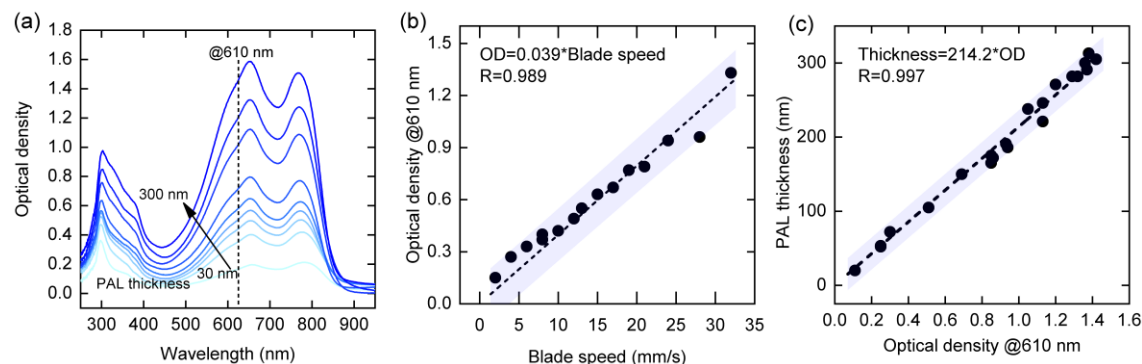


Fig. S1. Thickness quantification of the bladed-coated films. (a) Optical density spectra as a function of the photoactive layer thickness (b) Optical density value at 610 nm as a function of the blade speed. (c) Thickness of the photoactive layer as a function of the optical density at 610 nm. Dashed lines and confidence band of 98% are plotted to guide the eye.

Table S1. Fine-tuned values for the laser patterning of P1, P2 and P3. The optical images of the screened laser parameter in Fig. S.

| Ablation step | Current (A) | Overlap (%) | Frequency (kHz) | Speed (mm/s) | Nominal line width (mm) | Pulse width (μs) |
|---------------|-------------|-------------|-----------------|--------------|-------------------------|------------------|
| P1 | 16-20 | 33 | 15 | 100 | 0.01 | 1 |
| P2 | 17.5-19 | 90 | 100 | 100 | 0.01 | 1 |
| P3 | 17-19 | 90 | 100 | 100 | 0.01 | 1 |

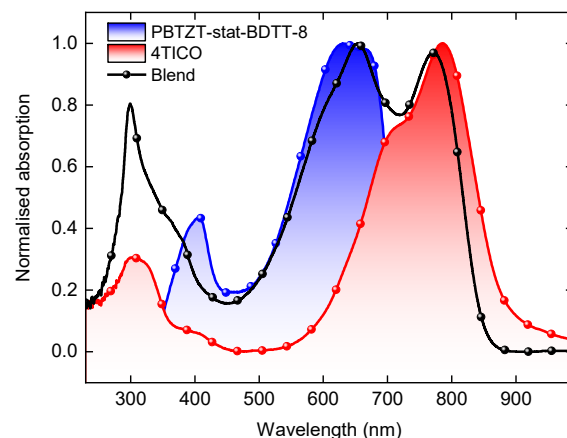


Fig. S2. Normalised absorption of PBTZT-stat-BDTT-8, 4TICO and blended materials.

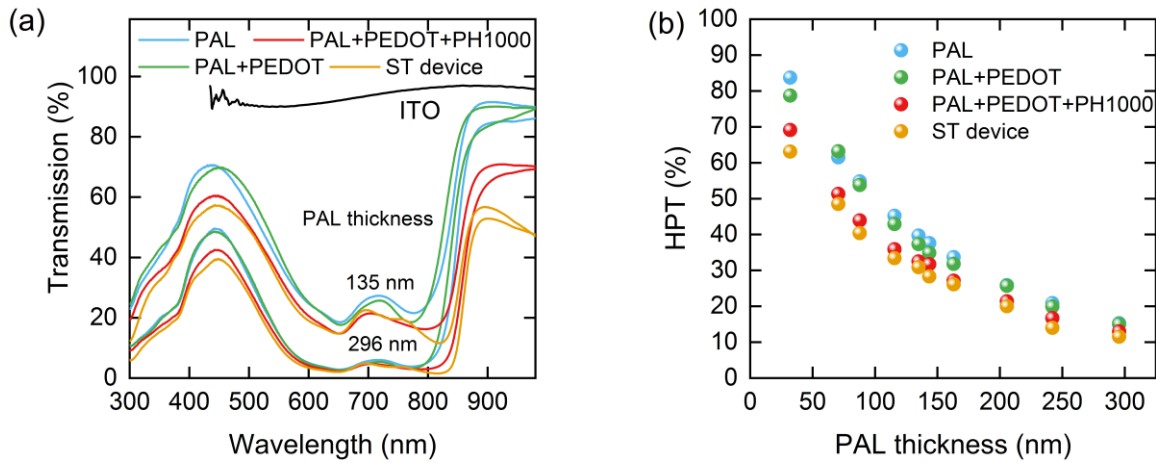


Fig. S3. Contribution to transparency of each layer: photoactive layer (PAL), PEDOT:PSS 4083, PEDOT PH1000 and full semitransparent device (ST device). (a) For two PAL thicknesses 135 nm and 296 nm. (b) Human perception transmittance (HPT) as a function of the PAL thickness for each layer.

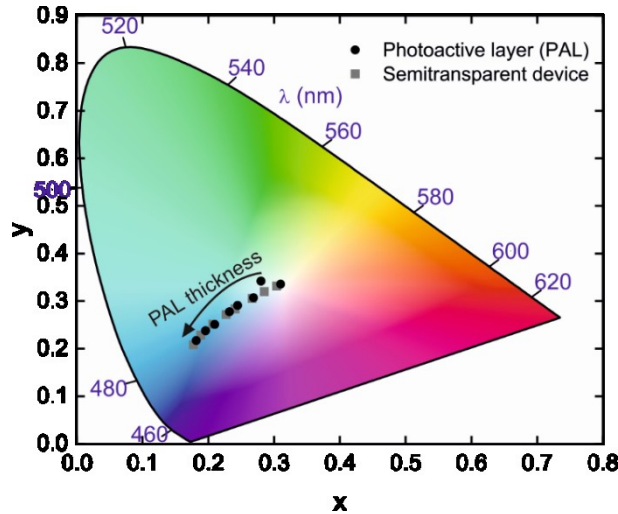


Fig. S4. Colour CIE coordinates of photoactive layer films (as depicted in Fig1b) and semitransparent device (with the contribution of electrodes).

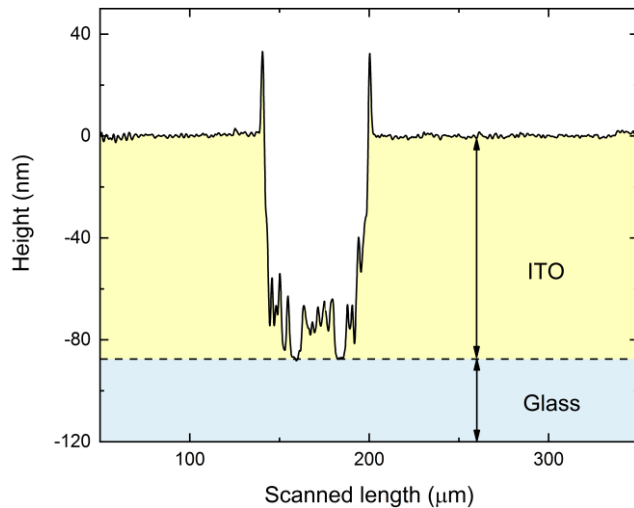


Fig. S5. Groove profile of the optimized P1 patterning extracted with the mechanical profilometer.

Table S2. Transparency metrics and colour characteristics of PBDTZT-stat-DBTT-8 and 4TICO films shown in Figure 1. Human perception transmittance (HPT) and average visual transmittance (AVT) are defined in Eq.1 and Eq. 2 of the main manuscript. Full device transparency highlighted in bold.

| Layers | PAL thickness (nm) | HPT (%) | AVT (%) | Transmission at 550 nm (%) | CIE coordinates (x,y) | Colour rendering index (CRI) |
|------------------|--------------------|-----------|-----------|----------------------------|-----------------------|------------------------------|
| ITO | 100 | 90.4 | 92.1 | 90 | (0.3289,0.3359) | 99.2 |
| PAL | 32 | 83.7 | 80.6 | 86 | (0.3102, 0.3352) | 98.4 |
| PAL+PEDOT | | 79 | 76 | 81 | (0.3127, 0.3363) | 98.1 |
| ST device | | 63 | 61 | 65 | (0.304, 0.3313) | 98.8 |
| PAL | 71 | 62 | 60 | 64 | (0.2803, 0.3416) | 97.3 |
| PAL+PEDOT | | 63.2 | 61.1 | 66 | (0.2931, 0.3253) | 98.4 |
| ST device | | 49 | 48 | 50 | (0.285, 0.3195) | 98.4 |
| PAL | 88 | 55 | 53 | 57 | (0.2687, 0.3070) | 95.2 |
| PAL+PEDOT | | 53.8 | 52.7 | 56 | (0.2814, 0.3161) | 97.3 |
| ST device | | 40 | 40 | 42 | (0.2667, 0.3052) | 96.0 |
| PAL | 135 | 40 | 39 | 42 | (0.2445, 0.2905) | 88.8 |
| PAL+PEDOT | | 37.3 | 38.7 | 38 | (0.2457, 0.2803) | 93.5 |
| ST device | | 31 | 32 | 32 | (0.2406, 0.2835) | 90.4 |
| PAL | 160 | 34 | 34 | 35 | (0.2321, 0.2774) | 86.4 |
| PAL+PEDOT | | 31.8 | 33.7 | 32 | (0.2288, 0.2657) | 87.9 |
| ST device | | 26 | 27 | 27 | (0.2273, 0.2713) | 86.5 |
| PAL | 200 | 26 | 27 | 26 | (0.2099, 0.2507) | 75.6 |
| PAL+PEDOT | | 25.7 | 27.3 | 26 | (0.2116, 0.2557) | 76.9 |
| ST device | | 20 | 22 | 20 | (0.2068, 0.2513) | 74.3 |
| PAL | 240 | 21 | 23 | 21 | (0.1959, 0.2373) | 66.1 |
| PAL+PEDOT | | 19.9 | 22 | 20 | (0.1987, 0.2393) | 68.4 |
| ST device | | 14 | 16 | 14 | (0.1884, 0.2284) | 61.3 |
| PAL | 300 | 15 | 18 | 15 | (0.1818, 0.2167) | 55.8 |
| PAL+PEDOT | | 15 | 17.9 | 14 | (0.1837, 0.2125) | 57.6 |
| ST device | | 12 | 14 | 11 | (0.1773, 0.2079) | 52.9 |

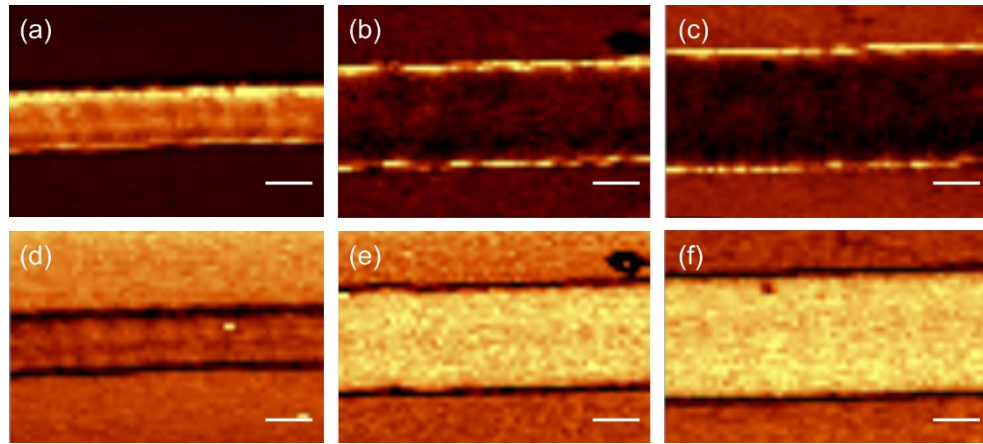


Fig. S6. Optimisation of P1 on ITO. Laser reflectivity at 785 nm (a, b, c) and PL (d, e, f) maps of laser patterned ITO with different laser ablation power: 16 A (a, d), 18 A (b, e) and 20 A (c, f). The laser measurement excitation was set to 785 nm. The white scale bar corresponds to 30 μm .

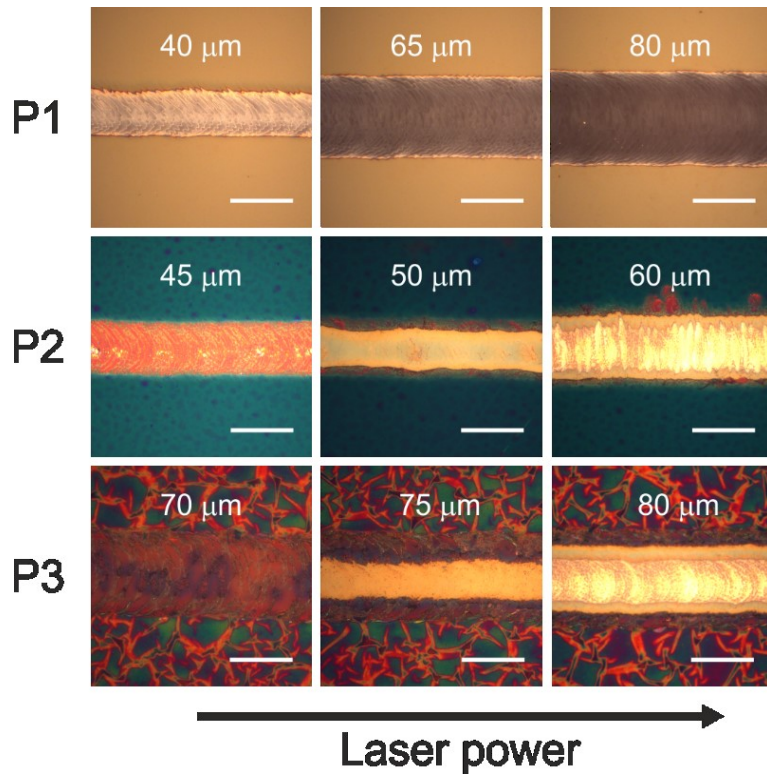


Fig. S7. Optimisation of laser patterning conditions. Microscope images of laser patterned lines with increasing laser excitation power, which results in an increase of the groove width (value inset in the pictures) for P1 (Glass/ITO), P2 (Glass/ITO/ETL/PAL/HTL) and P3 (Glass/ITO/ETL/PAL/HTL/PH1000). The rest of the laser parameters was fixed as mentioned in the experimental section. The central column corresponds to the optimized laser conditions with which modules were manufactured. The white scale bar corresponds to 50 μm .

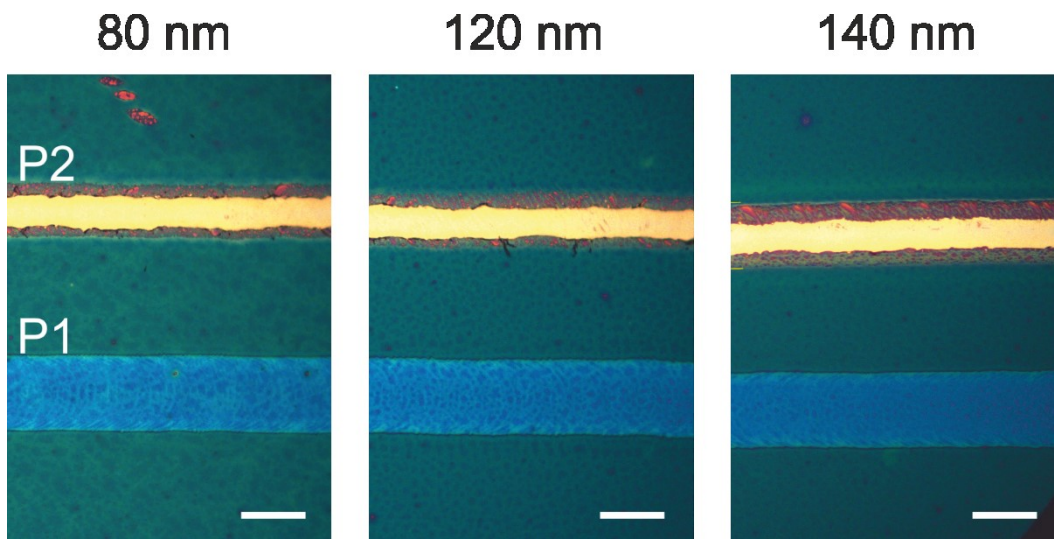


Fig. S8. Microscope image of the laser patterned organic films for photoactive layer thicknesses of 80, 120 and 140 nm. Scale bar is 50 μ m.

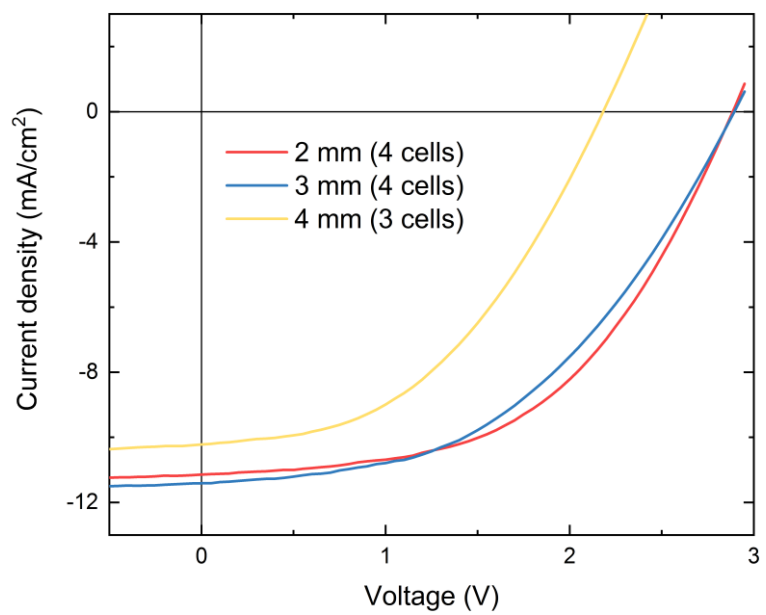


Fig. S9. JV characteristics of modules with 2, 3 and 4 mm cell length.

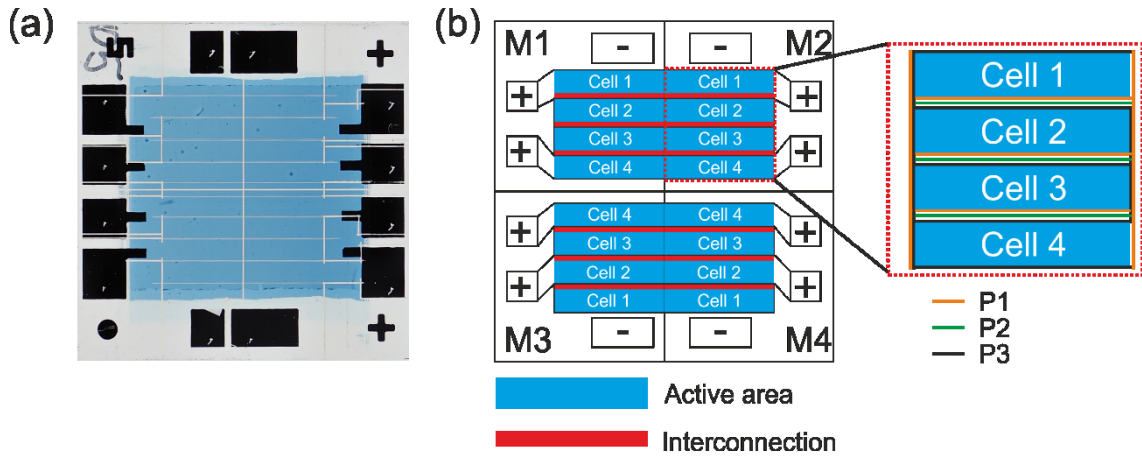


Fig. S10. Layout of the laser patterning design. (a) Photograph (5×5 cm) and (b) scheme of the modules layout with the detailed laser patterned grooves. The shown substrate on white background contains 4 different modules (M1-M4)

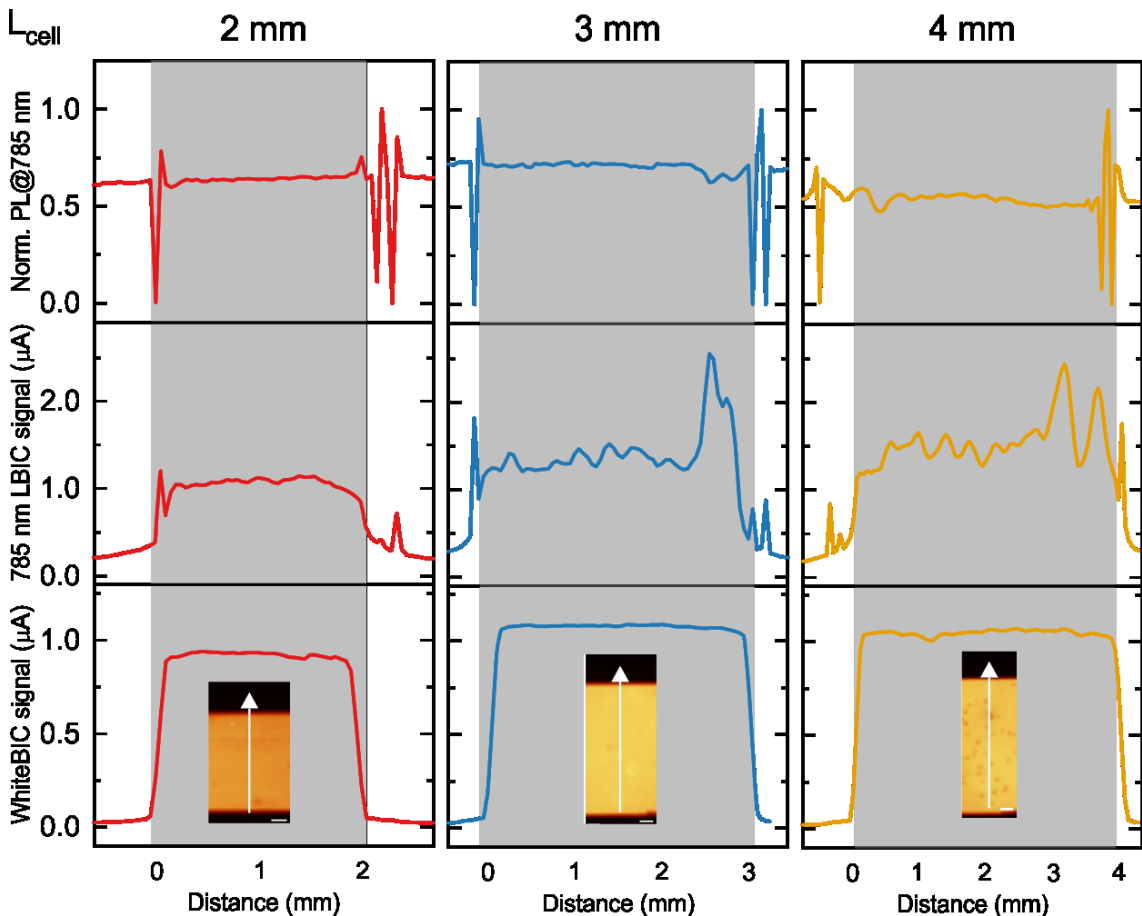


Fig. S11. Transversal image cross section of the normalized PL, 785 nm LBIC and whiteBIC maps for 2, 3 and 4 mm. L_{cell} module from Fig.5. Inset: whiteBIC maps with an arrow pointing the direction of the averaged cross section. The grey rectangle is a guide to identify the cell length.